

Elasticity of carbon allotropes. III. Hexagonal graphite: Review of data, previous calculations, and a fit to a modified anharmonic Keating model

C. S. G. Cousins

School of Physics, University of Exeter, Stocker Road, Exeter EX4 4QL, United Kingdom

M. I. Heggie

School of Chemistry, Physics and Environmental Science, University of Sussex, Falmer, Brighton BN1 9QJ, United Kingdom

(Received 10 May 2002; published 22 January 2003)

The experimental data relating to the second- and third-order elasticity and the zone-center optic modes of hexagonal graphite are reviewed and some amendments proposed. A modified Keating model involving three sets of interactions, one planar and two interlayer, has been developed. The harmonic parameters, four planar and seven interlayer, have been fitted by least-squares procedures to five second-order elastic constants, five zone-center optic-mode frequencies and two assumptions relating to internal strain. The anharmonic parameters comprise three planar and three interlayer ones. They have been fitted to the pressure derivatives of the five second-order constants and of three of the optic-mode frequencies. The full spectrum of inner elastic constants and internal strain tensors is given, the composition of the second- and third-order elastic constants is exposed, and the corresponding elastic compliances calculated. A pressure-induced phase transition is correctly predicted at around 16 GPa.

DOI: 10.1103/PhysRevB.67.024109

PACS number(s): 62.20.Dc, 63.20.-e, 81.40.Jj

I. INTRODUCTION

The formal aspects of the elasticity through third order of two diamond and two graphite allotropes of carbon have been presented in Refs. 1 and 2 (hereafter C1 and C2). In the first paper of the present sequence³ [paper I (C3)] attention was focused on cubic diamond (cD) and an optimized Keating model was developed whose parameters, four harmonic and five anharmonic, provide an excellent account of the elastic constants, pressure derivatives of the elastic constants, the frequency of the optic mode at the zone center, and the various phonon deformation parameters. In anticipating the application of the model to hexagonal diamond (hD) it was realized that, unlike valence force field models, the Keating model suffers from an infelicity of strain definition whereby the parameters of the model depend on a dimension of the chosen unit cell. A slight modification to the definition of strain removes the problem with the result that hD is very successfully handled in Paper II.⁴

The (almost?) exclusive use of the Keating formalism in connection with cubic diamond- and zinc-blende-structure materials has led to its identification as a model of the covalent bond. In fact there is no “physical” content in the Keating model—it is simply a way of associating strain derivatives of energy with the structural variables, interatomic separations and angles, that are thought likely to be significant for whatever reason. In this paper we have extended the modified Keating model to hexagonal graphite (hG).

The elasticity of hG is a challenge from both theoretical and experimental points of view on account of the extreme anisotropy of the structure. If the elasticity of cD is referred to Cartesian axes with Ox_1 \parallel $[1\bar{1}0]$ and Ox_3 \parallel $[111]$ the greater part of the resulting quasirhombohedral set of elastic constants (given in full in C3) may be compared directly to the hG set. Both the differences and the similarities are startling:

hG's C_{33} at 36.5 GPa is a mere 3% of its cD equivalent, 1215 GPa, while the combination that relates to uniform strain within layers, $C_{11} + C_{12}$, is 1240 GPa in hG and 1274 GPa in cD. Thus hG is as stiff as cD within a layer but 30 times more compliant between layers. A consequence of this is the ease with which irregularity of stacking can take place and accounts for the fact that single crystalline regions of natural graphite are always both limited in extent and contain a mixture of the hexagonal and rhombohedral forms. Such material cannot be used for ultrasonic determinations of elastic constants but, in powder form, can be compressed and changes in the lattice parameters followed by x-ray diffraction.^{5,6} In this way both second- and third-order compressibilities may be determined.

Second-order elastic constants may be obtained from ultrasonic experiments on compression-annealed pyrolytic graphite.⁷⁻⁹ This material consists of layers that are stacked with high precision (c axes parallel within 0.5°) but whose a axes are distributed at random. In spite of this it is still possible to find the single-crystal constants because second-order elasticity is isotropic in the basal plane, rendering the randomness invisible. This isotropy does not extend to the third-order elastic constants. Since the latter are usually measured by determining the uniaxial stress dependence of ultrasonic wave velocities through single crystals it is unlikely that they will be determined directly in the foreseeable future. Some combinations may be determined indirectly through the pressure dependence of the second-order constants, however.

The theoretical challenge arises from two sources. First there is the relative complexity of the structure. The basis consists of four atoms, none of which occupies a site with inversion symmetry. Thus, as shown in C1 and C2, there are numerous inner elastic constants besides the five independent second-order and ten independent third-order constants for a material belonging to Laue group HI. To extract a full

complement of components using any model in which the energy is not a simple function of interatomic separations, unit-cell volume, etc., requires the calculation of the energy for more than 280 000 configurations! This makes the development of a parametrization of the bonding in hG highly desirable.

Second there is the anisotropy. It is often reasonable in the case of close-packed structures, such as the fcc and the hcp, to fit Lennard-Jones potentials to second-order elastic constants and to transfer the parameters to defect situations. This cannot be done for hG: there is no way to define a pair potential that can represent a binding energy of 7 eV/atom and a nearest-neighbor distance 1.42 Å within a layer as well as the values 0.02 eV/atom and 3.35 Å between layers.¹⁰ To improve the situation an empirical potential for carbon invoking three-body contributions was introduced by Stillinger and Weber,¹¹ and Tersoff produced another that takes variable atomic coordination into account via a many-body term,¹² giving a reasonable account of the in-plane bonding. This was extended by Nordlund *et al.*,¹³ who added an interaction to accommodate the weak interlayer bonding. A further development, due to Heggie,¹⁴ resulted in a carbon potential capable of interpolating smoothly between sp^2 and sp^3 configurations. Part of this potential involved Keating-like terms, though these were limited to just the bond-stretching and bond-bending ones of the original¹⁵ model. As the development and optimization of a Keating model has been so successful for cD,^{3,15-18} it was felt worthwhile to extend the ideas to hG. As indicated in Ref. 3 this model is semiclassical, quasiharmonic and slightly approximate in that it ignores the distinction between adiabatic and isothermal elastic constants. Any discrepancies are likely to be very small at modest temperatures. The elastic constants fall into two groups: one contributed to principally by the sp^2 -bonding interactions within the graphene planes and the other by π bonding between planes.

In Sec. II we review the experimental data and justify our model. The development of the model is carried out in Sec. III and the fitting and the results are presented and discussed in Sec. IV.

II. MODELING THE ELASTICITY

A. Appraisal of input data

1. At the second order

The five second-order elastic constants of pyrolytic graphite were determined by Blakslee *et al.*⁷ and three of these are taken as target values here. Revised values are used for C_{13} and C_{44} .

The reported values for C_{44} ranged from 0.18 to 0.35 GPa and are very small. They arise from the anomalously low velocities of transverse ultrasonic waves propagated along the c axis and stem from the mobility of dislocations. When the latter is eliminated by neutron irradiation values up to 5 GPa are found. The high values are believed to be characteristic of ideal single-crystal material. Sensitivity to the state of the crystal has been demonstrated by Grimsditch¹⁹ using Brillouin surface scattering. He confirms the value 5.05

± 0.35 GPa found earlier for a sample of natural graphite²⁰ and confirms also what appeared at first sight to be a contradictory value 3.25 ± 0.015 GPa, reported in Ref. 21 for highly oriented pyrolytic graphite. The difference is consistent with the influence of crystallite grain size on the speed of surface waves. The higher value has been adopted here.

Zhao and Spain²² used their compressibility data to probe the linear modulus $B_a (\equiv 1/k_a)$ and presented a case for raising the value of C_{13} from 15 GPa to 22 ± 2 GPa. Unfortunately they inadvertently used the expression for the planar modulus! If their procedure is carried through correctly the value of C_{13} is lowered to 7.9 ± 3.5 GPa.

Five of the six zone-center optic-mode frequencies are known, of which two can be converted directly to inner elastic constant values. The E_{1u} mode^{23,24} at 1587 cm^{-1} (47.58 THz) gives $E_{11}^{12} = 253.0 \text{ GPa \AA}^{-2}$ and the A_{2u} mode²⁵ at 868 cm^{-1} (26.0 THz) gives $E_{33}^{12} = 75.66 \text{ GPa \AA}^{-2}$.

2. At the third order

The anharmonic part of the potential determines the nonlinear part of the compressibility and the pressure derivatives of the second-order constants and of the zone-center optic-mode frequencies.

We have taken the early work on the compressibility of graphite carried out by Lynch and Drickamer⁶ and fitted their tabulated values of a/a_0 and c/c_0 to quartics in p . We find for the linear compressibilities $k_a = 14.4 \times 10^{-4} \text{ GPa}^{-1}$ and $k_c = 2.24 \times 10^{-2} \text{ GPa}^{-1}$. The former value is high compared to that derived by inversion of the C_{IJ} , $6.4 \times 10^{-4} \text{ GPa}^{-1}$, and casts some doubt on the $a(p)$ measurements. The value of k_c is much closer to the inversion value of $2.7 \times 10^{-2} \text{ GPa}^{-1}$. Other experiments^{7,8} gave $(2.68 \pm 0.13) \times 10^{-2} \text{ GPa}^{-1}$ and $(2.4 \pm 0.2) \times 10^{-2} \text{ GPa}^{-1}$. The nonlinear compressibilities are $K_a = 2.8 \times 10^{-4} \text{ GPa}^{-2}$ and $K_c = 4.66 \times 10^{-3} \text{ GPa}^{-2}$. This value of K_a is actually rather large and indicates a perceptible nonlinearity in the in-plane compressibility. Kelly²⁶ observes that this nonlinear variation of a cannot be correct in the light of the work of Hershbach and Laurie,²⁷ in which indirect information on the anharmonicity of planar bonds is obtained by analyzing C-C bond force constants. Zhao and Spain²² reported that the pressures in Ref. 6 are probably overestimated increasingly with higher pressure, thereby introducing the suspect nonlinearity into the pressure dependence of a . Their own work showed no such behavior.

A more recent study of finely ground natural graphite by Hanfland *et al.*²⁸ presents compressibility data via a one-dimensional analog of the Murnaghan equation of state:²⁹

$$r/r_0 = [(\beta'/\beta_0)p + 1]^{-1/\beta'}$$

where r is a or c , $\beta_0^{-1} = -(d \ln r/dp)_{p=0} = k_r$ is the linear compressibility and β' is the pressure derivative of β . The values $k_a = 8.0 \times 10^{-4} \text{ GPa}^{-1}$ and $k_c = 2.8 \times 10^{-2} \text{ GPa}^{-1}$ are implied. Expansion of the above expression to second order in p leads to the identification

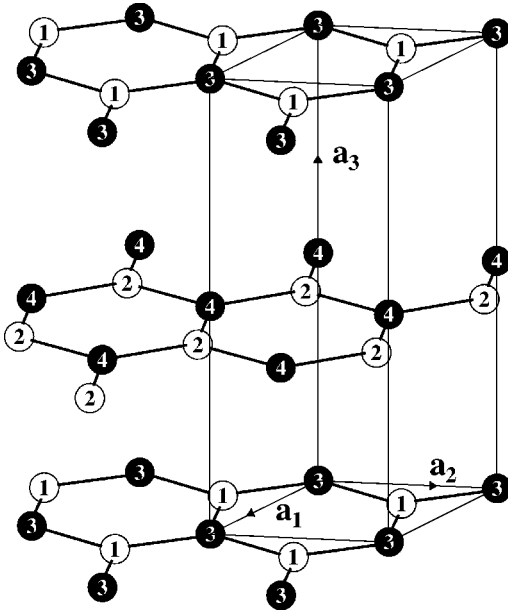


FIG. 1. A unit cell of the crystal structure of hG.

$$\beta' = -2 + \frac{K_r}{k_r^2}$$

and their value of 10.8 for β' when $r=c$ then implies that $K_c = 10.0 \times 10^{-3} \text{ GPa}^{-2}$.

The full set of pressure derivatives of second-order elastic constants was presented by Gauster and Fritz.⁹ The value of C'_{44} at 0.0023 was problematic, like C_{44} , a victim of dislocation mobility. A later study⁸ reassesses the derivative to be 0.81 ± 0.15 and also raises the earlier value of C'_{33} from 9.6 to 14.6 ± 1.1 .

The Raman shifts under pressure of the E_{2g} modes have been measured²⁸ and yield $d\omega/dp$ of 0.140 and 0.145 $\text{THz} (\text{GPa})^{-1}$ for the E_{2g2} and E_{2g1} modes, respectively. Similar measurement³⁰ on the B_{1g1} mode gives $d\omega/dp = 0.572 \text{ THz} ((\text{GPa})^{-1})$.

B. Justification of model

As indicated in the Introduction it is the large anisotropy of graphite that makes the modeling of elastic constants particularly difficult. Most early work, as reviewed in Kelly,²⁶ concentrated on explaining the interlayer constants, C_{33} , C_{44} , and their pressure derivatives. In particular the experimental work of Blakslee *et al.*⁷ and Green *et al.*⁸ was followed by theoretical studies using, first, simple pairwise potentials (Lennard-Jones and exponential core) in Ref. 31 and, second, parabolic and other band models for the electronic contributions to the constants in Ref. 32.

In an unpublished investigation we have used the Ewald summation technique³³ to calculate the full spectrum of contributions to elastic and inner elastic constants through third order for all inverse powers of atomic separation from $n = 4$ to $n = 14$. It was impossible (i) to combine any two of these in such a way that the structure was in equilibrium at the observed lattice parameters, i.e., with the first-order con-

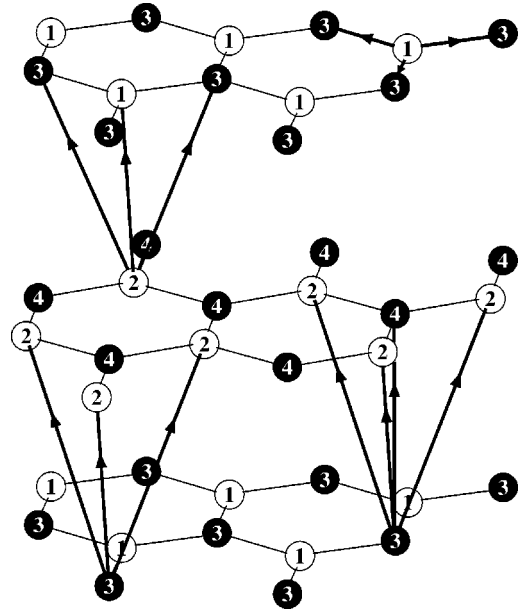


FIG. 2. Configurations of bonds in the Keating model. Filled atoms are Bernal type A, empty atoms are type B. Upper right: three in-plane BA bonds. Lower right: an AA' and three AB' bonds. Lower left: three AB' bonds. Upper left: a BB' and two BA' bonds. The associated interactions are described in the text.

stants C_1 and C_3 simultaneously zero, or (ii) to combine any three in such a way that $C_1 = C_3 = 0$ without C_{33} being negative and C_{44} always far too small or negative. In addition all zone-center optic-mode frequencies involving the $E_{33}^{\lambda\mu}$ were imaginary.

The notion that elastic constants may be simulated by *any* combination of pair potentials can be ruled out by reference to one of the two second-order Cauchy relations. Central forces within the graphene planes imply $C_{11}^0 = 3C_{12}^0$. The observed values are $C_{11} = C_{11}^0 - \Delta = 1060 \text{ GPa}$ and $C_{12} = C_{12}^0 + \Delta = 180 \text{ GPa}$, where Δ is the internal strain contribution. This gives $C_{11}^0 = 930 \text{ GPa}$, $C_{12}^0 = 310 \text{ GPa}$, and $\Delta = -130 \text{ GPa}$. A value of $|\Delta|$ equal to 40% of C_{12}^0 is unreasonably large, implying enormous internal strain in total contrast to cD where it is very small. Thus we expect strong noncentral forces within the layers. The second relation is $C_{13} = C_{44}$. As shown above the relevant values are $C_{13} = 7.9 \pm 3.5 \text{ GPa}$ and $C_{44} = 5.05 \pm 0.35 \text{ GPa}$. Within the large experimental error the Cauchy relation is satisfied although the quoted value of C_{13} exceeds that of C_{44} by 57%. We therefore suspect and assume the presence of weak noncentral forces between the layers.

Nemanich *et al.*²⁵ who reported an experimental determination of the A_{2u} mode frequency, 868 cm^{-1} , drew attention to previous calculations based on various force field models in which frequencies in a wide range from 600 to 1300 cm^{-1} were predicted. They asserted that the nature of the lattice dynamics of graphite is such that even a valence force model with bond-stretching, bond-bending, and three-body terms cannot describe the A_{2u} mode: a four-body force, characterized by a puckering of the layer planes, is required. We have not found this problem with the model developed here.

TABLE I. The SWMcC model parameters γ_i (data and attribution taken from Ref. 40) and the bond interactions selected for the Keating model.

γ_i	Value (eV)	Arising from	Bond stretching	Bond bending
γ_0	2.598	AB and BA in-plane interactions	AB BA	AB/AB BA/BA
γ_1	0.364	AA' interlayer interactions (determines width of π bands at the K point)	AA'	AA'/AB'
γ_4	0.177	AB' and BA' interlayer interactions	AB'BA'	AB'/AB' BA'/BA'
γ_3	0.319	BB' interlayer interactions	BB'	BB'/BA'
γ_5	0.036	AA'' alternate layer interactions		
γ_2	-0.014	BB'' alternate layer interactions (determines π band overlap)		
γ_6	-0.026	Chemical shift between A and B atoms		

Nemanich *et al.*²³ measured the E_{2g_2} frequency as well as that of the E_{1u} mode and found the splitting between them to be 150 GHz. They argued that to fit the $\omega(E_{1u}) > \omega(E_{2g_2})$ observation it is necessary to include second-nearest-neighbor out-of-plane interactions, a conclusion supported by Al-Jishi and Dresselhaus in their lattice-dynamical model.³⁴ Such interactions are included in this development.

III. MODIFIED KEATING MODEL

The structure of hG is shown in Fig. 1 and fully described in C1. Briefly, the basis consists of two sets of two atoms occupying inequivalent sites. Their position coordinates and the indices assigned to their related sublattices are shown in Table I in C1. We shall also use Bernal notation³⁵ in which

TABLE II. Target data for the harmonic part of the modified Keating model. Units are GPa for C_{IJ} and GPa \AA^{-2} for $E_{ii}^{\lambda\mu}$.

	Experiment	Assumed	Fit
C_{13}	7.9 ± 3.5 ^a		7.9
C_{33}	36.5 ± 1.0 ^b		36.5
C_{44}	5.05 ± 0.35 ^c		5.05
E_{33}^{12}	75.66 ± 0.09 ^d		75.663
$E_{33}^{11} - E_{33}^{12} + E_{33}^{33}$		75.65	75.65
$\frac{1}{2}(C_{11}^0 + C_{12}^0)$	620 ± 28		620
$\frac{1}{2}(A_{16}^3 - A_{16}^1)$		-0.082	-0.082
" ζ_K "		0.115	0.115
C_{11}^0		1063.85	1063.85
C_{12}^0		176.15	176.15
C_{11}	1060 ± 20 ^b		1060
C_{12}	180 ± 20 ^b		180
E_{11}^{12}	253.0 ± 0.5 ^e		253.0
$E_{11}^{11} - E_{11}^{12} + E_{11}^{33}$	251.6 ± 0.5 ^e		251.6

^aRe-evaluation of conclusion drawn in Ref. 22.^bReference 7.^cReference 19.^dReference 25.^eReference 23.

the inequivalent sites are designated A (sublattices 3 and 4) and B (sublattices 1 and 2).

A. Strain variables

With four atoms in the basis the strain variables are more complicated than those of cD because of the three distinct inner displacement vectors $\vec{\zeta}^\lambda$. The strains may be expressed as

$$\Delta_{ii} = 2r_p^{i0} \eta_{pq} r_q^{i0} + 2r_p^{i0} z_p^\pi + z_p^\pi z_p^\pi \quad (1)$$

and

$$\Delta_{ij} = 2r_p^{i0} \eta_{pq} r_q^{j0} + r_p^{i0} z_p^\rho + r_p^{j0} z_p^\pi + z_p^\rho z_p^\pi, \quad (2)$$

where terms of order three and higher have been omitted and the significance of \vec{z}^π and \vec{z}^ρ is as follows. Consider the reference atom belonging to sublattice 2 in the central layer in Fig. 2. It has three bonds to atoms on sublattice 4 within the layer and four sets of three bonds to sublattices 1 and 3 in the layers above and below. When i refers to sublattice 1 $\vec{z}^\pi = -\vec{\zeta}^1$ (minus because a positive value indicates 2 relative to 1, 3 relative to 2 or 1, or 4 relative to 3, 2, or 1). Similarly when i refers to sublattice 3 $\vec{z}^\pi = +\vec{\zeta}^2$ and when it refers to sublattice 4 then $\vec{z}^\pi = \vec{\zeta}^2 + \vec{\zeta}^3$ because "4 relative to 2" is equivalent to "3 relative to 2" plus "4 relative to 3," similarly for j and \vec{z}^ρ , and for the remaining reference atoms.

B. Model parameters

The electronic structure of graphite is successfully approached by the Slonczewski-Weiss-McClure (SWMcC) model³⁶⁻⁴⁰ and leads to a parametrization in which the energy of π bonding is associated with various vectors (AA', AB', BA', and BB') between adjacent layers, vectors (AA' and BB'') between alternate layers, and with the nearest-neighbor in-plane vectors (AB and BA). We reproduce in Table I the SWMcC parameters deduced by Charlier, Gonze, and Michenaud⁴⁰ in their first-principles study of the electronic properties of hG, together with a brief indication of the significance of these parameters, as given in their Appendix. This provides a guide to selecting specific sets of vectors to

TABLE III. Target data for the anharmonic part of the modified Keating model. Units are GPa^{-2} for the K_i and THz GPa^{-1} for the f' . The C'_{IJ} are dimensionless.

	Experiment	Assumed	Fit
C'_{13}	3.1 ± 0.5^a		3.05
C'_{33}	9.6 ± 0.8^a		
	15.2 ± 1.1^b	14.6	12.7
C'_{44}	0.81 ± 0.15^b		1.9
$f'(E_{2g1})$	0.145 ± 0.012^c		0.145
$f'(B_{1g1})$	0.572 ± 0.020^d		0.663
C'_{11}	39.0 ± 3.9^a		39.0
C'_{12}	11.0 ± 1.1^a		11.0
$f'(E_{2g2})$	0.140 ± 0.001^c		0.140
$10^6 K_a$	$282,^e 1.92^c$	O(5.8)	5.8
$10^3 K_c$	$4.66,^e 10.0^c$	O(10)	11.8

^aReference 9.

^bReference 22.

^cReference 28.

^dReference 30.

^eReference 6.

parametrize the elasticity of hG. Corresponding to the four largest parameters we focus initially on four sets: one planar and three interlayer.

(i) The planar part of the energy per cell is modeled analogously to cD. The three nearest-neighbor A atoms to a B atom, see upper right portion of Fig. 2, give rise to three two-body ‘‘bond-stretching’’ BA_i interactions, three three-body ‘‘bond-bending’’ $BA_i BA_j$ interactions and various couplings between them. The same number of interactions arise from each A atom. Up to four harmonic parameters (α , β , σ , and τ) and six anharmonic parameters (γ , δ , ϵ , η , θ , and ξ) may be needed here.

(ii) This set comprises the two-body AA'_i interaction between nearest neighbors in adjacent planes, see lower right portion of Fig. 2, and the three-body interactions that couple

the AA'_i with the three neighboring oblique interlayer vectors AB'_j . Up to ten more parameters may be needed (with superscript ‘’).

(iii) This set comprises the three two-body AB'_i interactions and the three three-body interactions involving $AB'_i AB'_j$ pairs, see lower left portion of Fig. 2, together with the symmetrical group of two-body BA'_i and three-body $BA'_i BA'_j$ interactions. Up to ten more parameters may be needed (with superscript ‘’).

(iv) This set comprises the three two-body BB'_i interaction between nearest neighbors in adjacent planes and the three-body interactions that couple each BB'_i with the two closest neighboring oblique interlayer vectors BA'_j , see upper left portion of Fig. 2.

These sets are also shown in Table I in line with the SWMcC parameters γ_i with which they are associated. The fourth set can be discarded, however, because of geometrical interdependence. This arises as follows. Starting and finishing at a B site there are several loops of four vectors, symbolically $BB' + B'A + AA' + A'B = 0$, which may be used to express all Δ_{ii} and Δ_{ij} belonging to set 4 in terms of the strain variables of the other three sets.

With a possible 12 harmonic and 18 anharmonic parameters arising from the remaining three sets we are loath to introduce the AA'' and BB'' interactions. In fact these involve vectors joining pairs of atoms on the same sublattice and their bond-stretching aspect thus makes no contribution to the inner elastic constants.

C. Energy

The three sets of parameters defined above, together with the bookkeeping, results in expressions considerably lengthier than those relating to cD.⁵ Not all terms are destined for use. In keeping with the streamlining introduced in the modified model the only coefficients that are not unity are the halves associated with terms that are counted twice in the summations over sublattices.

TABLE IV. The modified Keating parameters. Note the smaller units for the anharmonic interlayer parameters.

	Planar		Interlayer					
	$\text{GPa } \text{\AA}^{-1}$	$\text{eV } \text{\AA}^{-4}$		$\text{GPa } \text{\AA}^{-1}$	$\text{eV } \text{\AA}^{-4}$		$\text{GPa } \text{\AA}^{-1}$	$\text{eV } \text{\AA}^{-4}$
α	266.21	1.6615	α'	39.55	0.2469	α''	3.231	0.02016
β	240.53	1.5013	β'	3.005	0.01875	β''	0.289	0.00180
σ	30.12	0.1880	σ'	-5.035	-0.03143			
τ	53.50	0.3340	τ'	-6.120	-0.03820	τ''	1.445	0.00902
	$\text{GPa } \text{\AA}^{-3}$	$\text{eV } \text{\AA}^{-6}$		$\text{MPa } \text{\AA}^{-3}$	$\text{meV } \text{\AA}^{-6}$		$\text{MPa } \text{\AA}^{-3}$	$\text{meV } \text{\AA}^{-6}$
γ	-688.00	-4.2941	γ'	197.5	1.233	γ''	-35.87	-0.2239
δ	-965.44	-6.0258						
ϵ	-366.84	-2.2896				ξ''	-5.44	-0.0339

TABLE V. The inner elastic constants. The D tensors are in GPa \AA^{-1} , the E tensors in GPa \AA^{-2} , and the F tensors in GPa \AA^{-3} .

D_{16}^1	-19.5	D_{16}^3	20.0						
D_{136}^1	-2.4	D_{136}^3	-2.4						
D_{145}^1	-1.6	D_{145}^3	-1.6						
D_{211}^1	-6262	D_{211}^3	6262						
D_{222}^1	5440	D_{222}^3	-5439						
D_{314}^1	-2.4	D_{314}^3	-2.4						
E_{11}^{11}	253.0	E_{11}^{12}	253.0	E_{11}^{13}	0.93	E_{11}^{33}	251.6		
E_{33}^{11}	75.663	E_{33}^{12}	75.663	E_{33}^{13}	1.63	E_{33}^{33}	75.65		
E_{111}^{11}	-4569	E_{111}^{12}	-4569	E_{111}^{13}	5.9	E_{111}^{33}	-4581		
E_{112}^{11}	1082	E_{112}^{12}	1082	E_{112}^{13}	6.1	E_{112}^{33}	1070		
E_{113}^{11}	13.9	E_{113}^{12}	13.9	E_{113}^{13}	-1.7	E_{113}^{33}	13.9		
E_{135}^{11}	-3.3	E_{135}^{12}	-3.3	E_{135}^{13}	-3.3	E_{135}^{31}	-3.3	E_{135}^{33}	-3.3
E_{331}^{11}	114.9	E_{331}^{12}	114.9	E_{331}^{13}	1.0	E_{331}^{33}	103.0		
E_{333}^{11}	-42.3	E_{333}^{12}	-42.3	E_{333}^{13}	-57.9	E_{333}^{33}	25.7		
F_{112}^{111}	-773.4	F_{112}^{112}	-773.4	F_{112}^{113}	-0.15	F_{112}^{123}	-0.15		
F_{112}^{133}	-0.15	F_{112}^{223}	773.1	F_{112}^{333}	773.1				

1. Harmonic terms

The second-order energy per unit cell is

$$\begin{aligned}
 E^{(2)} = & \frac{1}{2} \sum_{s=1}^4 \sum_{i=1}^3 \left(\alpha \Delta_{ii}^2 + \sum_{j=1}^3 [\beta \Delta_{ij}^2 + \sigma (\Delta_{ii} + \Delta_{jj}) \Delta_{ij} \right. \\
 & + \tau \Delta_{ii} \Delta_{jj}] + \alpha'' \Delta_{ii}^2 + \sum_{j=1}^3 [\beta'' \Delta_{ij}^2 + \sigma'' (\Delta_{ii} + \Delta_{jj}) \Delta_{ij} \\
 & + \tau'' \Delta_{ii} \Delta_{jj}] \left. \right) + \sum_{s=3}^4 \sum_{i=1}^2 \left(\frac{1}{2} \alpha' \Delta_{ii}^2 + \sum_{j=1}^3 [\beta' \Delta_{ij}^2 \right. \\
 & \left. + \sigma' (\Delta_{ii} + \Delta_{jj}) \Delta_{ij} + \tau' \Delta_{ii} \Delta_{jj}] \right). \quad (3)
 \end{aligned}$$

2. Anharmonic terms

The third-order energy per unit cell is

TABLE VI. The internal strain tensors in \AA . The actual in-plane internal strain is given by $A_{iJ}^1 + A_{iJ}^2$ in one layer and by $A_{iJ}^2 + A_{iJ}^3$ in the other. These components are equal and opposite and the first of them is given in the fifth column.

iJ	A_{iJ}^1	A_{iJ}^2	A_{iJ}^3	$A_{iJ}^1 + A_{iJ}^2$
16	-1.21	1.29	-1.37	0.082
136	0.8	-0.8	0.8	0
145	7.4	-7.4	7.4	0
211	-53.7	78.2	-102.7	24.5
222	54.3	-79.2	104.1	-24.9
314	-1.2	1.2	-1.2	0

$$\begin{aligned}
 E^{(3)} = & \frac{1}{2} \sum_{s=1}^4 \sum_{i=1}^3 \left(\gamma \Delta_{ii}^3 + \sum_{j=1}^3 [\delta \Delta_{ij}^3 + \epsilon (\Delta_{ii} + \Delta_{jj}) \Delta_{ij}^2 \right. \\
 & + \eta (\Delta_{ii}^2 + \Delta_{jj}^2) \Delta_{ij} + \theta \Delta_{ii} \Delta_{ij} \Delta_{jj} + \xi \Delta_{ii} \Delta_{jj} (\Delta_{ii} + \Delta_{jj}) \\
 & + \gamma'' \Delta_{ii}^3 + \sum_{j=1}^3 [\delta'' \Delta_{ij}^3 + \epsilon'' (\Delta_{ii} + \Delta_{jj}) \Delta_{ij}^2 + \eta'' (\Delta_{ii}^2 \\
 & + \Delta_{jj}^2) \Delta_{ij} + \theta'' \Delta_{ii} \Delta_{ij} \Delta_{jj} + \xi'' \Delta_{ii} \Delta_{jj} (\Delta_{ii} + \Delta_{jj})] \left. \right) \\
 & + \sum_{s=3}^4 \sum_{i=1}^2 \left(\frac{1}{2} \gamma' \Delta_{ii}^3 + \sum_{j=1}^3 [\delta' \Delta_{ij}^3 + \epsilon' (\Delta_{ii} + \Delta_{jj}) \Delta_{ij}^2 \right. \\
 & + \eta' (\Delta_{ii}^2 + \Delta_{jj}^2) \Delta_{ij} + \theta' \Delta_{ii} \Delta_{ij} \Delta_{jj} + \xi' \Delta_{ii} \Delta_{jj} (\Delta_{ii} \\
 & \left. + \Delta_{jj}) \right). \quad (4)
 \end{aligned}$$

D. Elastic constants

Every independent elastic and inner elastic constant has been obtained in terms of these parameters by applying the generalized method of homogeneous deformation (described in C2) to a unit contribution of each Keating parameter in turn. Each of these numerous constants has many more terms than its cD counterpart: so instead of listing them as equations we have tabulated them in the Appendix.

IV. FIT AND THE RESULTS

As we possess only a limited amount of experimental data we cannot fit more than a few parameters. Even with an excellent match to all data there is no guarantee of unique-

TABLE VII. The composition of the calculated elastic stiffnesses and the corresponding compliances and compressibilities. Stiffnesses are in GPa, second-order compliances in TPa^{-1} , and third-order compliances in TPa^{-2} .

$IJ.$	Partial	$\leftarrow C_{IJ} \rightarrow$ Internal	Total	S_{IJ} Total
11	1063.85	-3.85	1060.0	0.973
12	176.15	3.85	180.0	-0.164
13	7.9		7.9	-0.175
33	36.5		36.5	27.47
44	5.05		5.05	198.0
			k_a	0.634
			k_c	27.1
			k_v	28.4
111	-8641.4	-3049.5	-11 690.5	7.0
113	-14.1	6.7	-7.4	-3.3
133	-120.0		-120.0	-1.4
333	-572.0		-572.0	11 765
144	-4.4	-4.2	-8.6	-214.7
244	-9.0	4.2	-4.8	-384.9
344	-74.7		-74.7	80 400
166	-5887.1	-899.7	-6786.8	34.9
266	2046.7	-1074.7	972.0	-10.6
366	-3.4	6.8	3.4	-5.7
			K_a	5.8
			K_c	11 752
			K_v	11 764

ness. At the second order the interlayer constants are fit first. The primary target data, see Table II, are C_{13} , C_{33} , C_{44} , and E_{33}^{12} , deduced from the frequency of the A_{2u} mode. In addition the combination $E_{33}^{11} - E_{33}^{12} + E_{33}^{33}$ is tentatively deduced from the values of the frequencies of the B_{1g1} and the B_{1g2} modes. No experimental value exists for the latter but in the lattice dynamical literature^{41,34} it is shown as nearly degenerate with the A_{2u} mode—so a close value has been assumed. Interlayer interactions are responsible for the splitting between the E_{1u} and E_{2g2} modes. A near-perfect fit is found by scanning possible sets of parameters interactively using MATHEMATICA software.⁴² The parameters so found contribute to both C_{11}^0 and C_{12}^0 . These values are subtracted from the observed values and, together with the frequency of the E_{1u} mode, are used to determine the planar parameters. A degree of freedom exists because the experimental data do not fix the (unknown) internal strain. In view of the extremely small value found in cD we set this arbitrarily so that $\frac{1}{2}(A_{16}^3 - A_{16}^1)$, which governs the in-plane inner displacement, was equal to -0.082 and equivalent to a quasi-Kleinman parameter ζ_K of 0.115. The harmonic parameters are listed in the upper part of Table IV.

The anharmonic parameters were fit by a similar process using the target data in Table III. The quality of the experimental data is mixed and it was very difficult at first to find a realistic fit at all. Eventual success depended on solving

two problems. The first of these occurred in the interlayer fit where a value near to zero was always predicted for f'_3 , the pressure dependence of the frequency of the E_{2g1} mode,²⁸ one of the more reliable pieces of experimental information. It was resolved when it was realized that C'_{44} and f'_3 have almost identical dependence on the Keating parameters and that a fit could be achieved by raising the target value of C'_{44} from 0.81 to 1.9 GPa, about 60% of C'_{13} . This appears to be totally reasonable in that C_{44} is about 60% of C_{13} . The quantities C'_{33} and f'_6 are similarly linked. Remarkably only three interlayer parameters are required and none of them involves bond bending. The second problem is the prediction of the third-order compressibilities K_a and K_c . The former is heavily dominated by C_{133} and the latter by C_{333} . Although these stiffnesses are fully determined by the interlayer parameters the planar fit has to be obtained before K_a and K_c can be found.

The planar fit is based on C'_{11} , C'_{12} , f'_2 , and K_a . These involve the six parameters in only four combinations: $2\gamma + \theta$, δ , $2\epsilon + \theta - 8\xi$, and $\eta + \theta - 4\xi$. In addition there is a linear relation between the four targets limiting the number of planar parameters to 3. We have set $\eta = \theta = \xi = 0$ and solved for γ , δ , and ϵ . This least-squares fit gives $K_a = -2 \times 10^{-6} \text{ GPa}^{-2}$. As there is no reliable value for K_a we have assumed that it will be similar to that of cD in view of

TABLE VIII. Zone-center optic modes. Experimental frequencies are given in both cm^{-1} and THz, the pressure derivatives in THz GPa^{-1} .

Mode(s)	Eigenvector(s)	Frequency f		Derivative df/dp	
		Experiment	Calculated	Experiment	Calculated
E_{1u}	$z_1^2 = 1, z_1^1 = z_1^3 = 0$ $z_2^2 = 1, z_2^1 = z_2^3 = 0$	1587 ^a	47.58	47.58	0.142
E_{2g_2}	$z_1^1 \approx -z_1^3 \approx \frac{1}{\sqrt{2}}, z_1^2 \approx 0$ $z_2^1 \approx -z_2^3 \approx \frac{1}{\sqrt{2}}, z_2^2 \approx 0$	1582 ^a	47.43	47.43	0.140 ^e
E_{2g_1}	$z_1^1 \approx -z_2^2 \approx z_1^3 \approx \frac{1}{\sqrt{3}}$ $z_2^1 \approx -z_2^2 \approx z_2^3 \approx \frac{1}{\sqrt{3}}$	42 ^b	1.26	1.41	0.145 ^e
A_{2u}	$z_3^2 = 1, z_3^1 = z_3^3 = 0$	868 ^c	26.02	26.02	-0.53
B_{1g_2}	$z_3^1 \approx -z_3^3 \approx \frac{1}{\sqrt{2}}, z_3^2 \approx 0$			25.74	-0.96
B_{1g_1}	$z_3^1 \approx -z_3^2 \approx z_3^3 \approx \frac{1}{\sqrt{3}}$	127 ^d	3.81	3.82	0.572 ^f

^aReference 24.^bReference 23.^cReference 25.^dReference 41.^eReference 28.^fReference 30.

the great similarity of the planar elasticity of hG to that of cD, to which attention was drawn in the Introduction. Since k_a proved to be 15% lower than its cubic counterpart we have chosen a similarly reduced target for K_a . This is easily reached by making very small adjustments to the interlayer parameters. Although this is a departure from the optimal least-squares fit it does not significantly affect the other targets. The results of the anharmonic fitting are summarized in the lower half of Table IV.

The most striking feature of the parameters overall is their relative size. The harmonic ones drop roughly an order of magnitude in going from set to set: α to α' to α'' , for example. While this is expected on the basis of the relative sizes of the various second-order elastic constants it is no guide to the startling anharmonic patterns. First the expected order-of-magnitude increase in passing from harmonic to anharmonic planar parameters, α to γ say, is totally reversed for the two interlayer sets. Second it appears that γ' is more than 3000 times smaller than γ implying that anharmonicity is almost exclusively a planar feature. Third the planar set has bond bending parameters of similar size to its bond-stretching ones in marked contrast to the interlayer sets where bond-stretching dominates.

The above fit translates into the inner elastic constants shown in Table V. These clearly reflect the contrast just noted between constants that involve the planar parameters and those that do not.

The internal strain tensors are shown in Table VI. The value of the linear internal strain was arbitrarily pre-selected. The components of the quadratic internal strain have been included because they follow directly from the inner elastic constants, as shown in C1. They do not affect elasticity below the fourth order. From a formal perspective they appear well behaved: for example the $A_{1JK}^1 + A_{1JK}^2$ are all zero. This is certainly to be expected as y components alone would be

involved in the relative displacement of sublattices if A and B sites were equivalent. The $A_{2JJ}^1 + A_{2JJ}^2$ are the only components that involve the planar parameters, hence their large values.

The decomposition of the elastic stiffnesses and compliances is shown in Table VII. The five second-order constants selected as targets came from various sources, including a re-analysis of a previously modified value of C_{13} . Their inversion therefore generates a different set of second-order compliances which, since the fitting procedure reproduced the experimental stiffnesses exactly, may be taken as the *de facto* experimental values also. Derived quantities, such as the compressibilities, follow directly, as shown in C2.

The spectrum of the third-order stiffnesses of hG is shown. The C_{JK} display the now-familiar planar/interlayer contrast. Whereas the magnitudes of the internal strain contributions to the second-order constants were from 0.4 to 2%, at the third order they range from 15 to 110%. On inversion to compliances just two components dominate, S_{333} and S_{344} , as did S_{33} and S_{44} at the second order. The great disparity between S_{333} on the one hand and S_{111} , S_{113} , and S_{133} on the other is precisely what is needed to achieve the disparity between K_a and K_c .

The zone-center optic-mode properties are shown in Table VIII. The modes and eigenvectors are described in C1. The two larger in-plane mode frequencies were targeted and there was no difficulty in reproducing the experimentally observed 150-GHz difference. In their Born-von Kármán lattice dynamical study,³⁴ Al-Jishi and Dresselhaus found, in agreement with Nemanich *et al.*,²³ that the above difference could be accounted for only by the inclusion of a second-neighbor interlayer interaction. They further added that all the zone-center frequencies and elastic constants, apart from C_{13} , could be fitted using only two interlayer and four planar neighborhoods. To fit both C_{13} , which they took to be 15

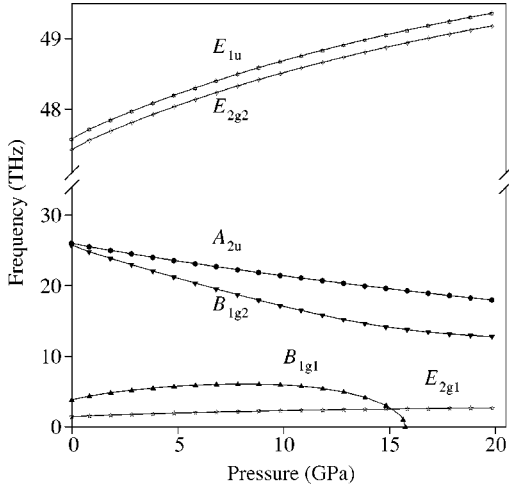


FIG. 3. Pressure dependence of the zone-center optic-mode frequencies.

GPa, and the frequency difference required extension to four interlayer neighborhoods. Whether the value of 7.9 GPa that has been used here would have improved their fit is unknown: what we have shown is that all the second-order elastic constants and zone-center frequencies can be fitted

using one planar and two interlayer sets of interactions.

The pressure derivatives of the frequencies were based on three experimental data, two of which were exactly matched with the third overestimated by 16%. Of the remaining three derivatives that of the E_{1u} mode is clearly very reasonable. The other two are larger in magnitude and opposite in sign. The actual variation of frequency with pressure for all the modes is shown in Fig. 3. These results are particularly satisfying because they characterize the behavior of a material approaching a pressure-induced phase transition: the axial modes A_{2u} and B_{1g2} show immediate softening while an initial hardening of B_{1g1} is followed by increasing softening from about 9 GPa. The frequency becomes zero, and the structure unstable, at 15.9 GPa. This value is perhaps a little high because of propagation of error from the overestimated value of the initial hardening.

Numerous investigations have shown that hG undergoes some sort of transition in just that range: Bundy and Kasper⁴³ achieved synthesis of hD by subjecting well-crystallized hG to a static pressure exceeding 13 GPa and a temperature above 1000 °C; Hanfland *et al.*²⁸ observed the E_{2g2} Raman line, noting a broadening that began at 9 GPa and the disappearance of the signal at 14 GPa; Yagi *et al.*⁴⁴ used a variety of high-pressure devices and synchrotron radiation to clarify structural details of the transition, finding that it occurred at

TABLE IX. Coefficients of the modified Keating parameters in the second-order partial and inner elastic constants. The common factors are expressed in terms of the lattice parameter a and the interlayer spacing d , with t standing for $\sqrt{3}$.

Factor	Planar				Interlayer: NN				Interlayer: NNN				
	α	β	σ	τ	α'	β'	σ'	τ'	α''	β''	σ''	τ''	
C_{11}^0	$2ta^2/3d$	1	1	-2	1					2	2	-4	2
C_{12}^0	$2ta^2/9d$	1	-1	-2	5					2	-2	-4	10
C_{13}	$4td/3$						2	2		4	-4	4	8
C_{33}	$16td^3/a^2$					$\frac{1}{3}$	2	4	2	2	4	8	4
C_{44}	$4td/3$						1	2		4	2	4	-4
D_{16}^1	$a/3d$	2	-2	-1	-2					4	-4	-2	-4
D_{16}^3	$a/3d$	-2	2	1	2			2		4	-4	-2	-4
E_{11}^{11}	$2t/3d$	2	1	2	-2					4	2	4	-4
E_{11}^{12}	$2t/3d$	2	1	2	-2					4	2	4	-4
E_{11}^{13}	$2t/3d$							1		4	2	4	-4
E_{11}^{33}	$2t/3d$	2	1	2	-2		2	2		4	2	4	-4
E_{33}^{11}	$4td/a^2$						1	2		4	8	16	8
E_{33}^{12}	$4td/a^2$						1	2		4	8	16	8
E_{33}^{13}	$4td/a^2$						2	4	2	4	8	16	8
E_{33}^{33}	$4td/a^2$					$\frac{4}{3}$	5	10	4	4	8	16	8
$E_{111,112,331}^{11(2)}$	$2t/3d$	2	-2	2	4					4	-4	4	8
$E_{111,112,331}^{12(2)}$	$2t/3d$	2	-2	2	4					4	-4	4	8
$E_{111,112,331}^{13(2)}$	$2t/3d$							1		4	-4	4	8
$E_{111,112,331}^{33(2)}$	$2t/3d$	2	-2	2	4			2	4	4	-4	4	8
$E_{113,333}^{11(2)}$	$8td/a^2$							1	1	2	4	8	4
$E_{113,333}^{12(2)}$	$8td/a^2$							1	1	2	4	8	4
$E_{113,333}^{13(2)}$	$8td/a^2$						1	2	1	2	4	8	4
$E_{113,333}^{33(2)}$	$8td/a^2$					$\frac{2}{3}$	2	5	3	2	4	8	4

TABLE X. Coefficients of the modified Keating parameters in the third-order partial elastic constants and the D and F tensors. Common factors expressed as in Table IX.

Factor	Planar						Interlayer: NN						Interlayer: NNN					
	γ	δ	ϵ	η	θ	ξ	γ'	δ'	ϵ'	η'	θ'	ξ'	γ''	δ''	ϵ''	η''	θ''	ξ''
C_{111}^0	ta^4/d	1	-1	2	-2	-1	2						2	-2	4	-4	-2	4
C_{113}^0	$8ta^2d/3$								1	1			3	3	-2		-1	8
C_{133}	$32td^3/3$							1	2	1	3		3	-3		6	3	12
C_{333}	$32td^5/a^2$						1	6	12	6	12		6	12	24	24	12	24
C_{144}^0	$2ta^2d/9$								1	4			12	-12	-6		12	24
C_{244}^0	$2ta^2d/3$								1	4			12		2		4	-8
C_{344}	$8td^3/3$							3	6	8	2	4	12	6	12	24		
C_{166}^0	$ta^4/9d$	3		2	-6	1	-2						6		4	-12	2	-4
C_{266}^0	$ta^4/9d$	1	-4	6	-2	-3	2						2	-8	12	-4	-6	4
C_{366}^0	$8ta^2d/9$									1	1		3	6			-3	
D_{136}^1	$4ad/3$									2	2		6	-6	-6	6	-3	
D_{136}^3	$4ad/3$								2	4	1	2	6	-6	-6	6	-3	
D_{145}^1	$2ad/3$								1	4			12	-3	-6	12	-12	-24
D_{145}^3	$2ad/3$							3	5	8			12	-3	-6	12	-12	-24
D_{211}^1	$a^3/3d$	3	3	-2	-3	-1	2						6	6	-4	-6	-2	4
D_{211}^3	$a^3/3d$	-3	-3	2	3	1	-2			2			6	6	-4	-6	-2	4
D_{222}^1	$a^3/3d$	-5	-1	2	5	-1	2						-10	-2	4	10	-2	4
D_{222}^3	$a^3/3d$	5	1	-2	-5	1	-2			$-\frac{10}{3}$			-10	-2	4	10	-2	4
D_{314}^1	$2ad/3$								1	4			12	-12	-12	12	-6	
D_{314}^3	$2ad/3$								3	8	2	8	12	-12	-12	12	-6	
F_{112}^{111}	$a/3d$	12	-3	-6	12	-12	-24						24	-6	-12	24	-24	-48
F_{112}^{112}	$a/3d$	12	-3	-6	12	-12	-24						24	-6	-12	24	-24	-48
F_{112}^{113}	$a/3d$									4			24	-6	-12	24	-24	-48
F_{112}^{123}	$a/3d$									4			24	-6	-12	24	-24	-48
F_{112}^{133}	$a/3d$								2	8			24	-6	-12	24	-24	-48
F_{112}^{223}	$a/3d$	-12	3	6	-12	12	24				8		24	-6	-12	24	-24	-48
F_{112}^{333}	$a/3d$	-12	3	6	-12	12	24	6	6	12			24	-6	-12	24	-24	-48

about 14 GPa and that the martensitically transformed phase was hD.

V. DISCUSSION

A widely used alternative to valence force field or Keating models is the Tersoff potential for carbon.¹² Its parametrization was undertaken by optimizing a large number of cohesive energies of carbon polytypes, vacancy formation energies, together with the lattice constant and the bulk modulus of cD. The emphasis was thus on energy rather than energy derivatives. Recently an interlayer potential of the Tersoff type was proposed for graphite in Ref. 13. We have tested this modified energy algorithm by incorporating it in our scheme in place of the Keating energy algorithm. The results were poor. For example C_{11} was down by 60%, C_{12} was very negative, and C_{33} was down by 75%. In addition C_{13} and C_{44} were essentially zero and some zone-center frequencies were imaginary, results indicating insufficient bond-bending content in the interlayer modification. This highlights the importance of having realistic energy derivatives.

The Keating model is a simple vehicle for carrying such derivatives through third order. We have extended the model

with rigor to a noncubic structure. As a preliminary it was necessary to review experimental data and an erroneous modification to C_{13} was identified and corrected. The parametrization is compact and involves only the nearest neighbors within a layer and the nearest- and next-nearest neighbors between layers. The quality of the harmonic fitting is very good, there was no difficulty in achieving a convincing fit, though it must be borne in mind that the fit is not unique. The planar parameters have substantial bond-bending character, qualitatively similar to those of cD (see C3), while the interlayer ones are biased in favor of bond stretching.

A single target C'_{44} had to be changed (from 0.81 to 1.9) in order to obtain any credible anharmonic fitting. The final result is particularly impressive in three respects. First it gives a good account of the pressure dependence of the remaining four second-order elastic constants, three optic-mode frequencies, and the two third-order compressibilities in terms of just six parameters, only one more than was necessary for cD. Second the huge contrast between the sizes of the planar and the interlayer parameters emphasises the difference between the covalent, strongly angularly dependent, planar interaction and the weak, almost central, inter-

TABLE XI. Coefficients of the modified Keating parameters in the third-order E tensors. Common factors expressed as in Table IX.

	Factor	Planar						Interlayer: NN						Interlayer: NNN					
		γ	δ	ϵ	η	θ	ξ	γ'	δ'	ϵ'	η'	θ'	ξ'	γ''	δ''	ϵ''	η''	θ''	ξ''
$E_{111}^{11(3)}$	$ta^2/3d$	6		1		2	-4							12		2		4	-8
$E_{111}^{12(3)}$	$ta^2/3d$	6		1		2	-4							12		2		4	-8
$E_{111}^{13(3)}$	$ta^2/3d$													12		2		4	-8
$E_{111}^{33(3)}$	$ta^2/3d$	6		1		2	-4							12		2		4	-8
$E_{112}^{11(3)}$	$ta^2/9d$	6	-6	-3		6	12							12	-12	-6		12	24
$E_{112}^{12(3)}$	$ta^2/9d$	6	-6	-3		6	12							12	-12	-6		12	24
$E_{112}^{13(3)}$	$ta^2/9d$									2				12	-12	-6		12	24
$E_{112}^{33(3)}$	$ta^2/9d$	6	-6	-3		6	12			2	4			12	-12	-6		12	24
$E_{113}^{11(3)}$	$4td/3$									4		4		12	6	12	24		
$E_{113}^{12(3)}$	$4td/3$									4		4		12	6	12	24		
$E_{113}^{13(3)}$	$4td/3$									2	6	1	4	12	6	12	24		
$E_{113}^{33(3)}$	$4td/3$							6	8	8	2	4		12	6	12	24		
$E_{135}^{11(3)}$	$2td/3$									2	8			24	12	24	48		
$E_{135}^{12(3)}$	$2td/3$									2	8			24	12	24	48		
$E_{135}^{13(3)}$	$2td/3$									4	12	2	8	24	12	24	48		
$E_{135}^{31(3)}$	$2td/3$							3	6	12				24	12	24	48		
$E_{135}^{33(3)}$	$2td/3$							9	16	16	6	8		24	12	24	48		
$E_{331}^{11(3)}$	$4td/3$									1	4			12	-12		24	12	48
$E_{331}^{12(3)}$	$4td/3$									1	4			12	-12		24	12	48
$E_{331}^{13(3)}$	$4td/3$									2	6	1	4	12	-12		24	12	48
$E_{331}^{33(3)}$	$4td/3$									5	8	6	16	12	-12		24	12	48
$E_{333}^{11(3)}$	$8td^3/a^2$							3	6	8	2	4		12	24	48	48	24	48
$E_{333}^{12(3)}$	$8td^3/a^2$							3	6	8	2	4		12	24	48	48	24	48
$E_{333}^{13(3)}$	$8td^3/a^2$							6	12	12	6	12		12	24	48	48	24	48
$E_{333}^{33(3)}$	$8td^3/a^2$							4	15	30	32	14	28	12	24	48	48	24	48

layer interaction. Third because of its clear indication of the pressure-induced phase transition.

At first sight it appears paradoxical that the *linear* variation of a (small K_a) and the *quadratic* variation of c (large K_c) as functions of pressure⁶ should be associated with the *strong* planar and *weak* interlayer anharmonicities, respectively. The paradox arises in the inversion of third-order stiffnesses to compliances and stems from the strong anisotropy of hG. Because C_{111} is so much larger than C_{333} the reciprocal nature of the inversion makes S_{111} very much smaller than S_{333} and so on. Thus K_c is dominated by *planar* anharmonicity, K_a by *interlayer* anharmonicity and the paradox is resolved. This argument will apply to other layer structures, such as hBN.

In the fourth paper⁴⁵ (Paper IV) of this sequence the model developed here is applied to rhombohedral graphite and includes a study of the postulated rG-to-cD transformation.

ACKNOWLEDGMENT

We are grateful to British Energy Generation Ltd. (formerly Nuclear Electric Ltd.), Barnwood, Gloucester, UK for financial support.

APPENDIX: ELASTIC CONSTANTS IN THE MODIFIED KEATING MODEL

Each constant M_i is written as a linear combination of Keating parameters K_j with coefficients μ_j and a common factor F_i : $M_i = F_i \times \sum \mu_j K_j$. The second-order constants appear in Table IX and the third-order ones in Tables X and XI. The common factors in these tables have been expressed in terms of the interlayer spacing d rather than the lattice parameter c to facilitate comparison with the treatment of rG in Ref. 45.

¹C. S. G. Cousins, J. Phys.: Condens. Matter **14**, 5091 (2002).

²C. S. G. Cousins, J. Phys.: Condens. Matter **14**, 5115 (2002).

³C. S. G. Cousins, Phys. Rev. B **67**, 024107 (2003).

⁴C. S. G. Cousins, Phys. Rev. B **67**, 024108 (2003).

⁵S. S. Kabalkina and L. F. Vereshchagin, Dokl. Akad. Nauk. SSSR **131**, 300 (1960) [Sov. Phys. Dokl. **5**, 373 (1960)].

⁶R. W. Lynch and H. G. Drickamer, J. Chem. Phys. **44**, 181 (1966).

- ⁷O. L. Blakslee, D. G. Proctor, E. J. Seldin, G. B. Spence, and T. Weng, *J. Appl. Phys.* **41**, 3373 (1970).
- ⁸J. F. Green, P. Bolsaitis, and I. L. Spain, *J. Phys. Chem. Solids* **34**, 1927 (1973).
- ⁹W. B. Gauster and I. J. Fritz, *J. Appl. Phys.* **45**, 3309 (1974).
- ¹⁰J.-C. Charlier, X. Gonze, and J.-P. Michenaud, *Europhys. Lett.* **28**, 403 (1994).
- ¹¹F. H. Stillinger and T. A. Weber, *Phys. Rev. B* **31**, 5262 (1985).
- ¹²J. Tersoff, *Phys. Rev. Lett.* **61**, 2879 (1988); *Phys. Rev. B* **39**, 5566 (1989).
- ¹³K. Nordlund, J. Keinonen, and T. Mattila, *Phys. Rev. Lett.* **77**, 699 (1996).
- ¹⁴M. I. Heggie, *J. Phys.: Condens. Matter* **3**, 3065 (1991).
- ¹⁵P. N. Keating, *Phys. Rev.* **145**, 637 (1966).
- ¹⁶P. N. Keating, *Phys. Rev.* **149**, 674 (1966).
- ¹⁷M. H. Grimsditch, E. Anastassakis, and M. Cardona, *Phys. Rev. B* **18**, 901 (1978).
- ¹⁸E. Anastassakis, A. Cantarero, and M. Cardona, *Phys. Rev. B* **41**, 7529 (1990).
- ¹⁹M. Grimsditch, *Phys. Status Solidi B* **193**, K9 (1996).
- ²⁰M. Grimsditch, *J. Phys. C* **16**, L143 (1983).
- ²¹S. A. Lee and S. M. Lindsay, *Phys. Status Solidi B* **157**, K83 (1990).
- ²²You Xiang Zhao and I. L. Spain, *Phys. Rev. B* **40**, 993 (1989).
- ²³R. J. Nemanich, G. Lucovsky, and S. A. Solin, in *Proceedings of the International Conference on Lattice Dynamics*, edited by M. Balkanski (Flammarion, Paris, 1975).
- ²⁴R. J. Nemanich, G. Lucovsky, and S. A. Solin, *Mater. Sci. Eng.* **31**, 157 (1977).
- ²⁵R. J. Nemanich, G. Lucovsky, and S. A. Solin, *Solid State Commun.* **23**, 117 (1977).
- ²⁶B. T. Kelly, *Physics of Graphite* (Applied Science Publishers, London, 1981).
- ²⁷D. R. Hershbach and V. W. Laurie, *J. Chem. Phys.* **35**, 458 (1961).
- ²⁸M. Hanfland, H. Beister, and K. Syassen, *Phys. Rev. B* **39**, 12 598 (1989).
- ²⁹F. D. Murnaghan, *Proc. Natl. Acad. Sci. U.S.A.* **30**, 244 (1944).
- ³⁰B. Alzyab, C. H. Perry, C. Zahopoulos, O. A. Pringle, and R. M. Nicklow, *Phys. Rev. B* **38**, 1544 (1988).
- ³¹J. F. Green and I. L. Spain, *J. Phys. Chem. Solids* **34**, 2177 (1973).
- ³²J. F. Green and I. L. Spain, *Phys. Rev. B* **11**, 3935 (1975).
- ³³P. P. Ewald, *Ann. Phys. (Leipzig)* **64**, 253 (1921).
- ³⁴R. Al-Jishi and G. Dresselhaus, *Phys. Rev. B* **26**, 4514 (1982).
- ³⁵J. D. Bernal, *Proc. R. Soc. London, Ser. A* **106**, 749 (1924).
- ³⁶J. C. Slonczewski and P. R. Weiss, *Phys. Rev.* **99**, 636(A) (1955); **109**, 272 (1958).
- ³⁷J. W. McClure, *Phys. Rev.* **108**, 612 (1967).
- ³⁸R. O. Dillon, I. L. Spain, and J. W. McClure, *J. Phys. Chem. Solids* **38**, 635 (1977).
- ³⁹R. C. Tatar and S. Rabii, *Phys. Rev. B* **25**, 4126 (1982).
- ⁴⁰J.-C. Charlier, X. Gonze, and J.-P. Michenaud, *Phys. Rev. B* **43**, 4579 (1991).
- ⁴¹R. Nicklow, N. Wakabayashi, and H. G. Smith, *Phys. Rev. B* **5**, 4951 (1972).
- ⁴²Stephen Wolfram, *The Mathematica Book*, 4th ed. (Wolfram Media/Cambridge University Press, Cambridge, England, 1999).
- ⁴³F. P. Bundy and J. S. Kasper, *J. Chem. Phys.* **46**, 3437 (1967).
- ⁴⁴T. Yagi, W. Utsumi, M. Yamakata, T. Kikegawa, and O. Shimomura, *Phys. Rev. B* **46**, 6031 (1992).
- ⁴⁵C. S. G. Cousins, *Phys. Rev. B* **67**, 024110 (2003).